NANO · MICRO small
www.small-journal.com

Check for updates

# Thermally Driven Transport and Relaxation Switching Self-Powered Electromagnetic Energy Conversion

*Maosheng Cao,* Xixi Wang, Wenqiang Cao, Xiaoyong Fang, Bo Wen, and Jie Yuan**

**Electromagnetic energy radiation is becoming a "health-killer" of living bodies, especially around industrial transformer substation and electricity pylon. Harvesting, converting, and storing waste energy for recycling are considered the ideal ways to control electromagnetic radiation. However, heat-generation and temperature-rising with performance degradation remain big problems. Herein, graphene-silica xerogel is dissected hierarchically from functions to "genes," thermally driven relaxation and charge transport, experimentally and theoretically, demonstrating a competitive synergy on energy conversion. A generic approach of "material genes sequencing" is proposed, tactfully transforming the negative effects of heat energy to superiority for switching self-powered and self-circulated electromagnetic devices, beneficial for waste energy harvesting, conversion, and storage. Graphene networks with "well-sequencing genes" ($w = P_c/P_p > 0.2$) can serve as nanogenerators, thermally promoting electromagnetic wave absorption by 250%, with broadened bandwidth covering the whole investigated frequency. This finding of nonionic energy conversion opens up an unexpected horizon for converting, storing, and reusing waste electromagnetic energy, providing the most promising way for governing electromagnetic pollution with self-powered and self-circulated electromagnetic devices.**

## 1. Introduction

Energy and environment is one of the hottest topics all over the world. Since last century, the rapid consumption of fossil fuels accompanied with environment pollution keeps plaguing human beings, and the consumption of fossil fuels will reach 27 terawatt-years in 2050. Searching for clean and renewed energy resources to satisfy increasing energy demand is the only way for sustainable development of human society. In 2007, Wang et al. proposed a direct-current nanogenerator by vertically aligned zinc oxide nanowire arrays, refreshing the horizon for energy generation and conversion.[1] Nanoenergy is considered as one of the most promising energy source, due to advantages of high output power, high energy conversion efficiency, and abundant material resources.[2] For example, Wang and Yang reported a hybridized electromagnetic–triboelectric nanogenerator, effectively converting wind energy by both of electromagnetic and triboelectric effects;[3] Chou and co-workers designed triboelectric–piezoelectric–electromagnetic hybrid nanogenerator to capture more energy of small mechanical disturbance in the environment.[4] Furthermore, amounts of efforts are continuously devoted to exploiting and updating methods for ambient energy harvest and conversion, such as thermal energy,[5] light energy,[6] water wave energy,[7] and most recently, electromagnetic energy is revealed.[8]

Over the past twenty years, electromagnetic energy has increasingly attracted attention, because of indispensability in various fields ranging from industrial manufacture to daily life, or even from national defense security to space exploration.[9–15] The growing amount of radiant energy, however, severely threat to human health. Investigating the electromagnetic energy harvest and conversion to govern electromagnetic pollution or even recycle the energy is becoming a hot spot around the world. Plenty of scientific researches have demonstrated that graphene is the most expected,[16–19] because of its fantastic properties including large specific surface area, high carrier concentration, and mobility with good mechanical properties.[20–22] Chen and co-workers indicated efficient shielding effectiveness (SE) by strong attenuation of graphene-based materials.[23] Later, Cao and co-workers reported the electromagnetic properties of dispersed graphene system at elevated temperature.[24] Especially, Cheng and and co-workers fabricated three-dimensional (3D) graphene foams and inflamed the researches into a new height with high efficiency and light weight.[25]

Nowadays, developing toward 3D/very-large-scale integration and miniaturization brings more challenges to electromagnetic energy conversion devices. Heat-generating and

Prof. M. S. Cao, Dr. X. X. Wang, W. Q. Cao
School of Materials Science and Engineering
Beijing Institute of Technology
Beijing 100081, China
E-mail: caomaosheng@bit.edu.cn
Prof. X. Y. Fang
School of Science
Yanshan University
Qinhuangdao 066004, China
Dr. B. Wen
Research School of Engineering
College of Engineering and Computer Science
The Australian National University
Canberra, ACT 2601, Australia
Prof. J. Yuan
School of Science
Minzu University of China
Beijing 100081, China
E-mail: yuanjie4000@sina.com
The ORCID identification number(s) for the author(s) of this article can be found under https://doi.org/10.1002/smll.201800987.

**DOI: 10.1002/smll.201800987**


© 2018 WILEY-VCH Verlag GmbH & Co. KGaA, Weinheim

temperature-rising during energy conversion is becoming an unneglectable problem, which causes performance degradation and harmful effect on stability and long life. More importantly, the heat-generating and temperature-rising obstructs harvesting and reusing of the waste electromagnetic energy around industrial transformer substation and electricity pylon where high power generates a large amount of heat energy.[8] Exploiting the way to eliminate the negative effect of heat energy remains a big problem.

In this work, a facile and universal approach of "material genes sequencing" is proposed for the first time, eliminating and even transforming the negative effect of heat energy to superiority for switching self-powered and self-circulated electromagnetic energy conversion devices. Different from previous reports,[3,4] it focuses on harvesting and converting the waste electromagnetic energy in the environment, providing the most promising way against the electromagnetic pollution. The electromagnetic energy is converted to heat energy, and the heat energy could be collected to drive thermoelectric power generator of electrical energy.[26] More importantly, the heat energy could further promote energy conversion with a favorable self-powered and self-circulated system (Figure S1, Supporting Information). A classical two-dimensional (2D) nanomaterial, graphene, is investigated as an example. Its thermally driven relaxation and charge transport are probed experimentally and theoretically, demonstrating a competitive synergy on electromagnetic energy conversion. A dynamic picture is successfully established to dissect from electromagnetic wave response to "material genes," generalizing the result further toward more 2D nanocrystals or others.

## 2. Results and Discussion

The link between material and electromagnetic functions is successfully analyzed in form and essence. We dissect hierarchically from electromagnetic wave response to "material genes," constructing a dynamic picture of electromagnetic

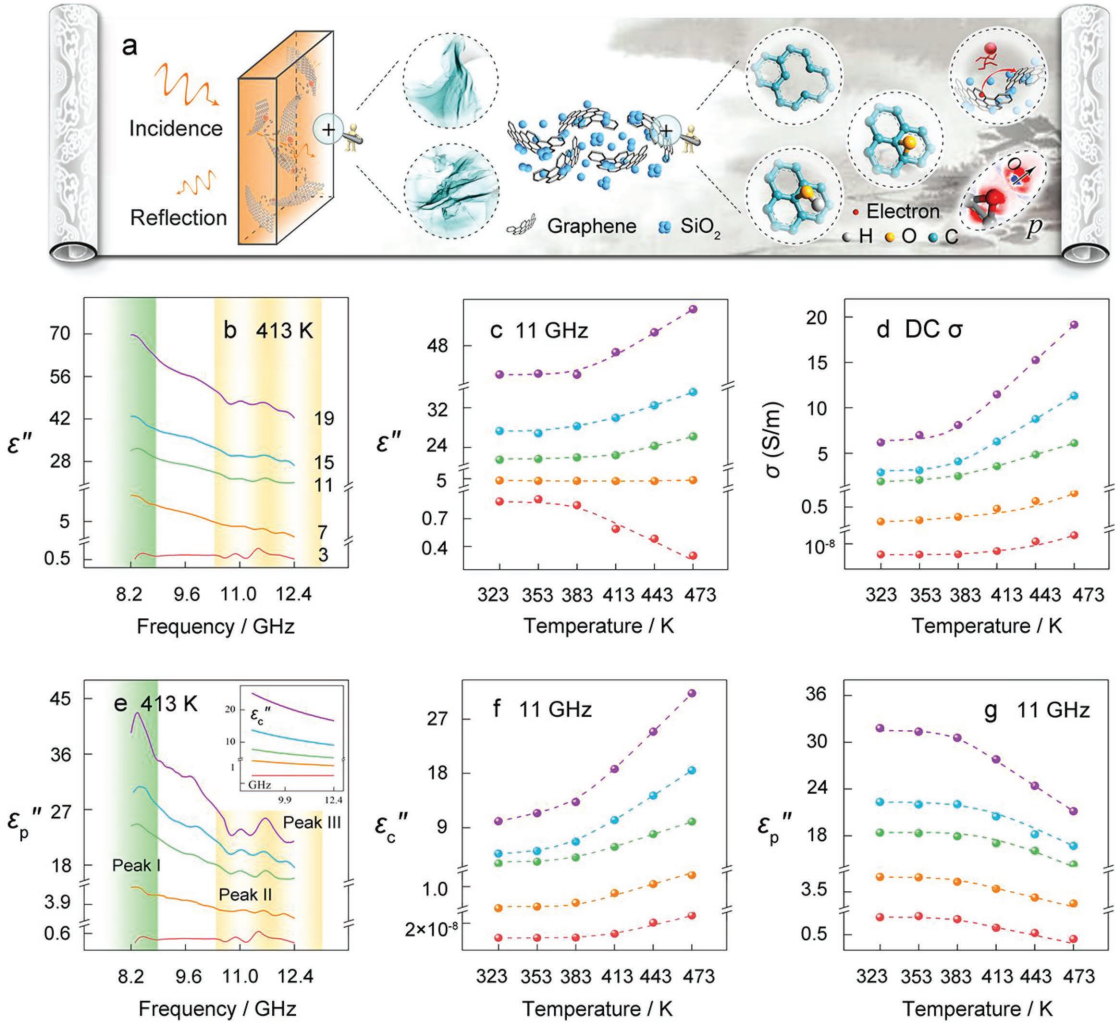


**Figure 1.** a) A scroll illustrating electromagnetic energy conversion of dispersed graphene in $SiO_2$, hierarchically dissecting from electromagnetic functions to "material genes," including morphology, lattice structure, electronic state, and organization structure. Frequency characteristics of b) $\varepsilon''$ and e) $\varepsilon_p''$ at $T = 413$ K, where $\varepsilon'' = \varepsilon_p'' + \varepsilon_c''$ (Inset: frequency characteristics of $\varepsilon_c''$ at $T = 413$ K). Temperature characteristics of c) $\varepsilon''$, f) $\varepsilon_c''$, and g) $\varepsilon_p''$ at $f = 11$ GHz, indicating the different thermally driven behaviors of energy loss contributed from charge transport and relaxation. It decides the distribution and conversion of electromagnetic energy. d) Temperature characteristics of $\sigma$.


© 2018 WILEY-VCH Verlag GmbH & Co. KGaA, Weinheim

energy harvest and conversion in graphene-silica xerogels ($SiO_2$) (**Figure 1**a; Figures S2–S4, Supporting Information).

The electromagentic wave repsonse is analyzed experimentally and theoretically. Figure 1b shows the imaginary permittivity ($\varepsilon''$) of graphene-$SiO_2$, which represents the loss factor of electromagnetic energy. They tend to decline with increase of frequency. Importantly, they present different temperature dependence: as graphene content is increased, temperature coefficients of $\varepsilon''$ change from negative to positive (Figure 1c). As well, it is insensitive to temperature at 7 wt% graphene content. This result suggests that for graphene-$SiO_2$, there is leakage conductivity ($\sigma$) thermally increasing, which makes contribution to $\varepsilon''$ as well as energy conversion. Further, the $\sigma$ is measured as shown in Figure 1d. It is enhanced directly by both temperature and graphene content. For characterizing energy conversion, the contributions of relaxation and charge transport to $\varepsilon''$ ($\varepsilon_p''$ and $\varepsilon_c''$, respectively) are separated. Three peaks appear near $f$ = 8.4, 11.0, and 11.6 GHz, indicating multiple relaxation in graphene-$SiO_2$ (Figure 1e; Figure S5, Supporting Information). The energy conversion by relaxation ($\varepsilon_p''$) is thermally weakened, while that by charge transport ($\varepsilon_c''$) is enhanced (Figure 1e,f). This opposite thermally driven behaviors of energy conversion exactly leads to different temperature coefficients of $\varepsilon''$.

Actually, $\varepsilon_p''$ mainly arises from polarization relaxation of defect dipoles and functional groups in graphene-$SiO_2$. **Figure 2**a presents a synthesis route of graphene. During the process, abundant functional groups, vacancy, and nonhexagonal-ring defects are implanted in/on graphene layers, as shown in Figure 2b–d.[27] Its selected area electron diffraction of graphene is shown in Figure S3 (Supporting Information), along the [001] zone axis. Two rings with *d*-spacing of 0.216 and 0.126 nm are observed corresponding to the (0–110) and (1–210) planes, accordant to results of previous literatures.[28] More than six bright hexagonal spots indicate that the graphene are of graphitic laminar structure of stacks, and it might contain clustered defects arising

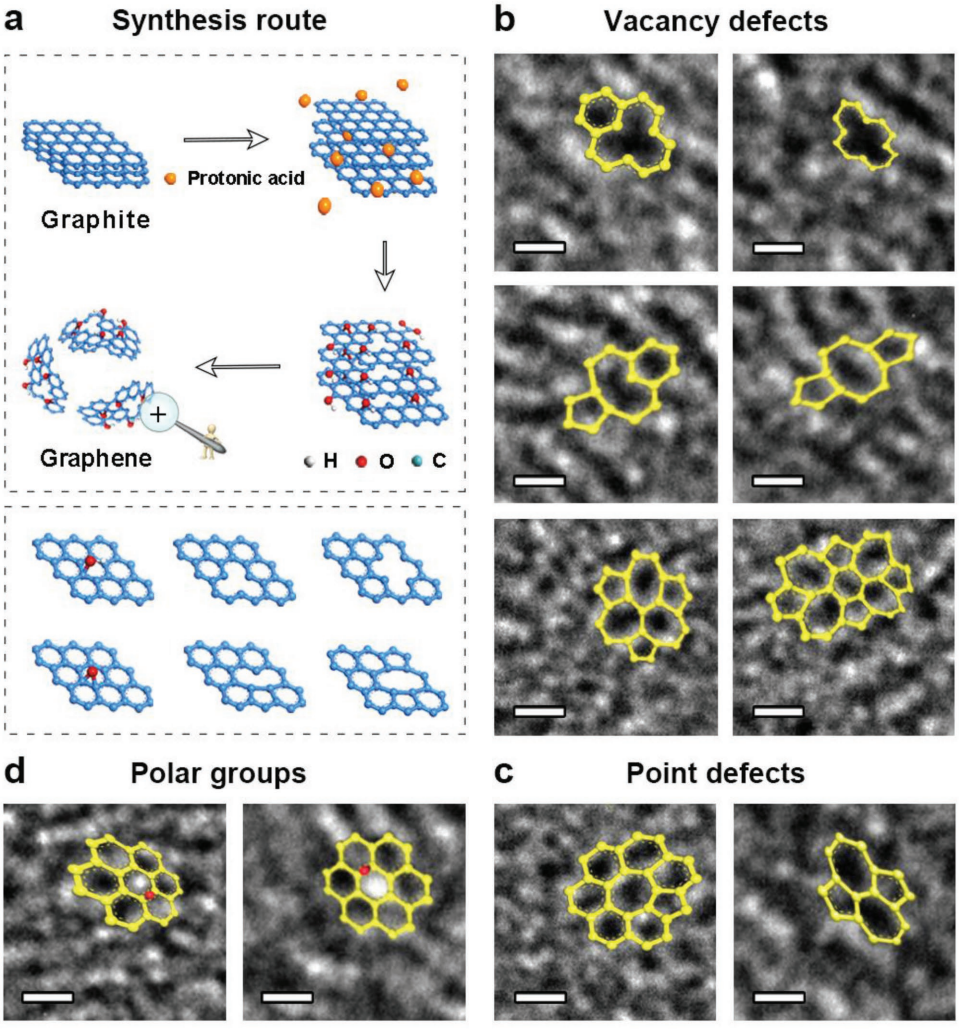


**Figure 2.** a) Schematic illustration for synthesis route of graphene, during which defects and groups are implanted in/on graphene layers. When graphene layers are dispersed in $SiO_2$, different "genomes" are sequenced affecting the thermally driven behaviors of energy conversion. b) HR-TEM images of graphene with various vacancy defects arising from lack of carbon atoms. c) HR-TEM images of graphene with point defects, arising from rotation of C—C bonds. d) HR-TEM images of graphene with groups. The scale bars are indexed to 1 nm.


© 2018 WILEY-VCH Verlag GmbH & Co. KGaA, Weinheim

from oxidation.[29] Their Fourier translation infrared (FT-IR) and X-ray photoelectron spectroscopy (XPS) spectra further confirm that graphene possesses abundant functional groups including hydroxyl (—OH), epoxy group (C—O—C), carbonyl (C=O) (Figure S6, Supporting Information). Meanwhile, XPS analysis indicates that over 80% of the functional groups are C—O, suggesting groups of the as-prepared graphene are mainly C—O—C and—OH, which is accordant with the results of FT-IR. According to the previous literatures, charge density differences at these structures appear asymmetric, indicating the formation of dipoles (Figure 1a).[30] Under alternating electromagnetic field, these dipoles will break loose, orientate, and convert electromagnetic energy into heat energy by relaxation.

Effect of temperature on relaxation is characterized by fitted relaxation time ($\tau$) in **Figure 3**a. According to Arrhenius model, $\tau$ is described as $\ln(\tau) = \ln(\tau_0) + U/kT$, where $U$ is activation of polarization, and $k$ is the Boltzmann constant of energy. The ln ($\tau$) of defect,—OH and C—O—C dipoles versus $T^{-1}$ are well fitted, with the slopes (l) in order, $l_D > l_{OH} > l_{COC} > 0$. It indicates the thermally driven decrease of $\tau$, attributed to the enhanced activity of dipoles. Under alternating electromagnetic field, these dipoles could rotate more easily with improved hysteresis and decreased frictional resistance, and meanwhile heat energy drives the depolarization of these dipoles, causing declined electromagnetic energy conversion power ($P_p$).

Effect of temperature on charge transport is shown in Figure 3b. The slopes of ln ($\sigma$) are in order, $l_3 < l_7 < l_{11} < l_{15} < l_{19} < 0$, manifesting the thermally driven enhancement of $\sigma$. More electrons will absorb energy, overcome resistance, and be activated to transport. It effectively promotes the electromagnetic energy conversion caused by conduction loss (Figure 1f). The conduction loss is codetermined by electron migrating and hopping in the conductive networks. They are regarded as "material genes" for energy conversion. Take graphene-$SiO_2$ as an example. Conductive network is failed to construct at low contents. As shown in Figure 3b, the potential barrier ($l_3$) is high, hindering electrons from hopping and transporting with very low $\sigma$ and $\varepsilon_c''$ as well as very low energy conversion power by charge transport ($P_c$). The slope order exhibits that conductive network is gradually improved with reduced

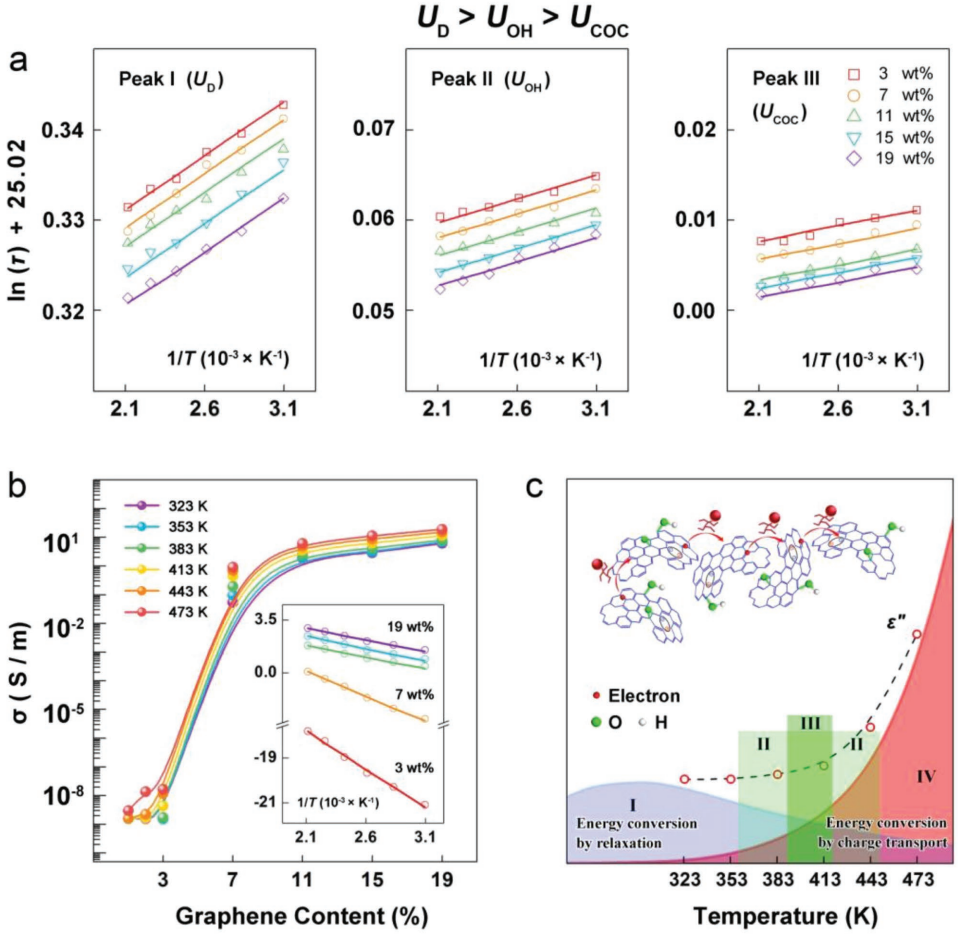


**Figure 3.** a) The ln ($\tau$) of relaxation peak I, II, and III versus $T^{-1}$, arising from defect dipoles,—OH and C—O—C, respectively. b) The $\sigma$ versus graphene content from 323 to 473 K (Inset: ln ($\sigma$) versus $T^{-1}$ where potential barrier of charge transport is directly proportional to absolute value of slope). c) Relationship of relaxation contributed $\varepsilon_p''$ and charge transport contributed $\varepsilon_c''$ versus temperature, where region I refers to domination of $\varepsilon_p''$, region II refers to synergy and competition of $\varepsilon_p''$ and $\varepsilon_c''$, region III refers to balance of $\varepsilon_p''$ and $\varepsilon_c''$, and region IV refers to domination of $\varepsilon_c''$. It demonstrates a competitive synergy of energy conversion contributed from relaxation and charge transport, implying the great potential for self-powered and self-circulated electromagnetic devices.


© 2018 WILEY-VCH Verlag GmbH & Co. KGaA, Weinheim

potential barriers by enhancing graphene content. Electrons then migrate and hop, leading to sharp increase of $\sigma$ and $\varepsilon_c''$ with ≈9 magnitude mutation.

The $\varepsilon''$ is codetermined by $\varepsilon_p''$ and $\varepsilon_c''$. Dipole relaxation at defects and functional groups are also considered as "genes" of materials. Figure 3c shows thermally driven relaxation and charge transport possess a competitive synergy on electromagnetic energy conversion. There are four regions: region I refers to domination of relaxation, where electron migrating and hopping are "frozen." Both electrons and dipoles are actived by heat energy. The reduced $\varepsilon_p''$ and increased $\varepsilon_c''$ will cause the synergy and competition of relaxation and transport in the region II, as well as balance in the region III. Finally, in the higher temperature region (region IV), electron transport do a major contribution to energy conversion.

Furthermore, the competitive synergy of relaxation and charge transport is influenced by "material genes sequencing." Low contents fail in conformation of graphene network with small $\sigma$. Dipole relaxation dominates the energy conversion, leading to location at region I. The effect of charge transport enables to be gradually improved by increasing the content, according to Figure 3b. It then compensates the decrease of relaxation loss, and shifts temperature region to cover from region I to III or IV. Therefore, "sequencing genes" of materials is greatly important to precise tuning of energy conversion. Just as "Genome Project," it could generalize the switching of self-powered and self-circulated electromagnetic energy conversion further toward more 2D nanocrystals or others.

Thermally driven electromagnetic energy harvest and conversion of graphene-$SiO_2$ is illustrated in **Figure 4**. On the graphene layers, abundant functional groups and defects cause the charge asymmetric distributions, inducing the formation of dipoles. These dipoles will rotate toward the electromagnetic field, converting electromagnetic energy to heat energy due to relaxation loss. Figure 4a shows that in local regions, graphene layers overlap tightly building conductive networks. Electrons could absorb electromagnetic energy to migrate in surface/interlayer channels, and then convert energy by colliding with the lattice.[31] Besides, electrons need to absorb more electromagnetic energy to hop across the potential barriers at the site of clustered functional groups or contact site of two graphene layers.[32] Affected by the afterheat, the energy conversion by relaxation loss is weakened perhaps due to depolarization, while that by conduction loss is strengthened because the variable range hopping and activated resistivity terms could be in series to account for the charge transport behavior.[32] Then, more electrons hop and network conductivity enhances, converting more electromagnetic energy to heat energy. Additionally, graphene-$SiO_2$ presents different thermally driven reflection behaviors. It is attributed to different impedance matching, influenced by charge transport on sample surface.

Figure 4b–e demonstrates that reflectivity and attenuation ($\alpha$, ability of energy conversion) are well tuned by thermally driven relaxation and transport. They promote the achievement of minimum reflectivity ($R$) at $T = 413$ K, and thermally increase it. Herein, ratio of energy conversion power contributed by charge transport and to that contributed by relaxation, $w = P_c/P_p$ is demonstrated to evaluate their competitive synergy on energy conversion. Figure 4c,d shows the double-coordinate 3D plots of $\alpha$ versus thermally driven $w$ and $\varepsilon'$. It is noticeable that when

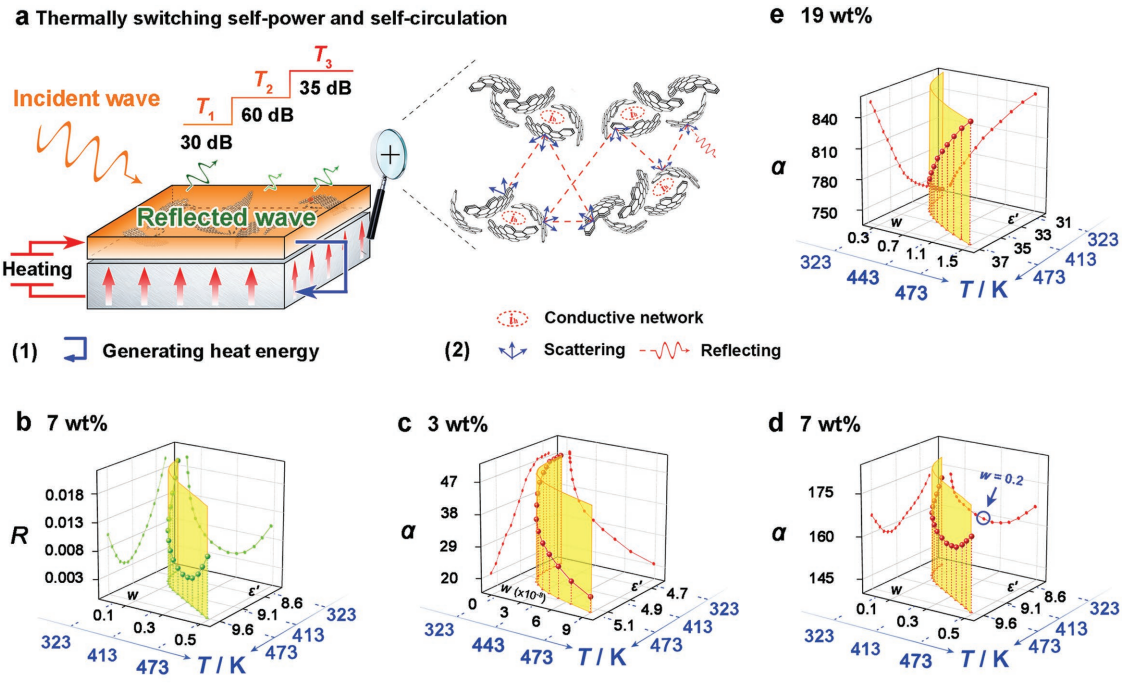


**Figure 4.** a) Schematic illustration for energy conversion of graphene-$SiO_2$ with self-powered and self-circulated system. Graphene networks, as nanogenerators, absorb electromagnetic energy, and convert it to heat energy, and meanwhile, the heat energy is reused to power graphene networks themselves promoting the energy conversion. b) Double-coordinate 3D plot of reflectivity versus thermally driven $w$ and $\varepsilon'$ at 7 wt%, $f = 11$ GHz and $d = 2.4$ mm. Double-coordinate 3D plots of $\alpha$ versus thermally driven $w$ and $\varepsilon'$ at c) 3 wt%, d) 7 wt%, and e) 19 wt% as well as at $f = 11$ GHz.


© 2018 WILEY-VCH Verlag GmbH & Co. KGaA, Weinheim

$w$ is over 0.2, $\alpha$ presents thermally increased tendency, while $w$ is lower than 0.2, $\alpha$ presents thermally decresed one (Figure S7, Supporting Information). Namely, "well-sequencing genes" could bring continuously enhanced electromagnetic attenuation with appropriate reflection. At that time, the graphene networks serve as nanogenerators, converting electromagnetic energy to heat energy and power themselves by afterheat energy, thermally promoting the energy conversion. This favorable self-circulation opens up a new way for harvesting, converting, and reusing excessive spread of electromagnetic energy around transformer substation and electricity pylon.

**Figure 5** shows the thermally turning electromagnetic functions for example. The multidimensional panorama analysis for electromagnetic wave absorption is shown in Figure 5a,b. There are multiple strong peaks at $T$ = 413 K. The maximum reaches ≈60 and 10 dB bandwidth almost covers X-band. Temperature also shifts absorption peaks and promotes 20 dB bandwidth over the whole investigated frequency (Figure 5c). Figure 5d,e show 3D search for electromagnetic shielding of graphene-$SiO_2$. It is directly proportional to temperature and graphene content with a mutation. The SE of 19 wt% graphene-$SiO_2$ full covers 34.8 dB and maximum reaches ≈39 dB.

The evaluation of thermally turning electromagnetic wave shielding and absorption is shown in Figure 5f (Figure S8, Supporting Information). Electromagnetic absorption is increased

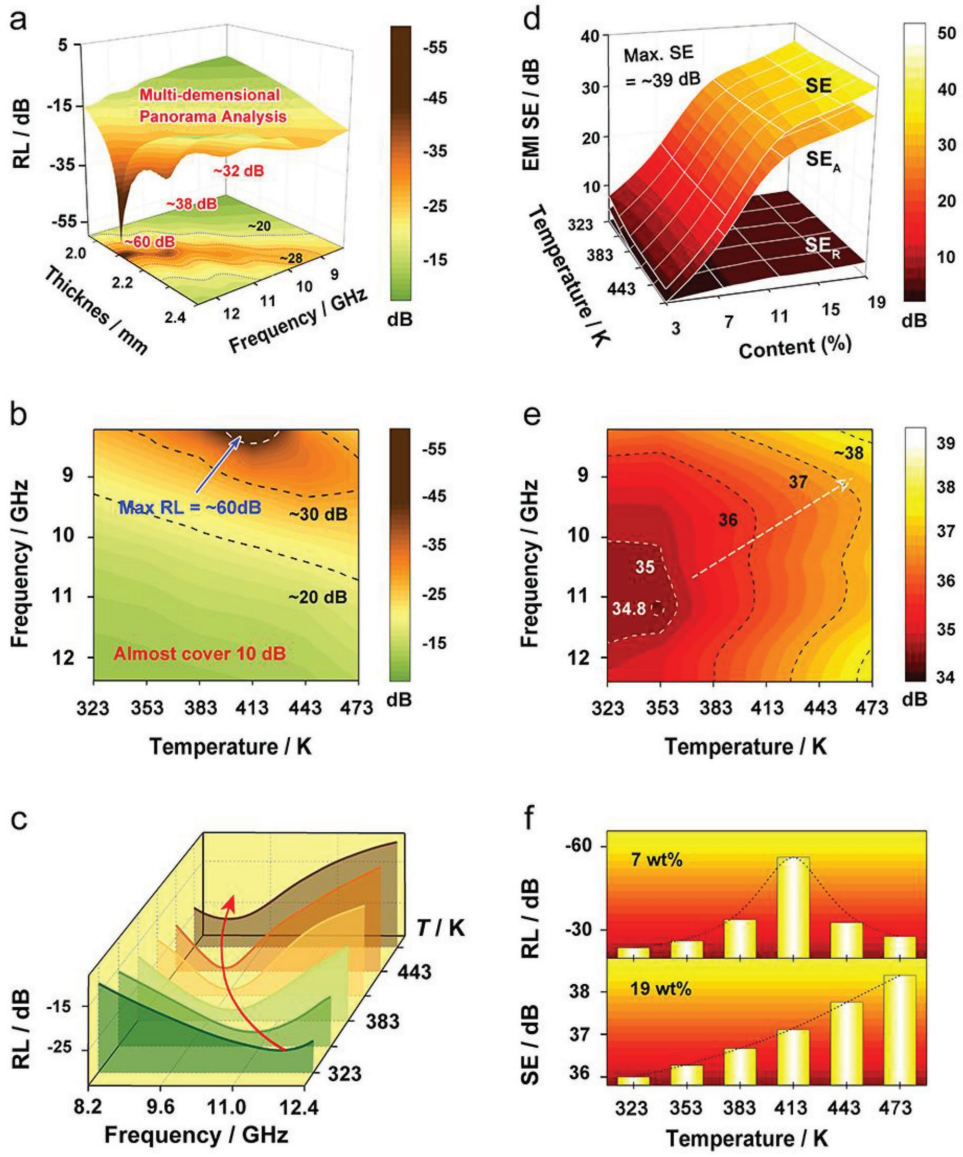


**Figure 5.** a) 3D plot of RL versus thickness and frequency at 7 wt% and $T$ = 413 K. b) 3D plot of RL versus temperature and frequency at 7 wt% and $d$ = 2.11 mm. c) RL versus frequency from 323 to 473 K at 7 wt% and $d$ = 2.33 mm. d) 3D plot of EMI SE, effective absorption contributed SE ($SE_A$) and reflection contributed SE ($SE_R$) versus temperature and graphene content. e) 3D plot of EMI SE versus temperature and frequency at 19 wt%. f) Statistics of maximal RL and maximal SE of 3–19 wt% graphene-$SiO_2$, indicating by "well-sequencing genes," electromagnetic functions could be thermally promoted by heat energy generated, forming a favorable self-powered and self-circulated electromagnetic devices.


© 2018 WILEY-VCH Verlag GmbH & Co. KGaA, Weinheim

by ≈250%, and shielding capacitor is constantly improved, demonstrating highly efficient and tunable electromagnetic functions in harsh environment. Based on "well-sequencing genes," the conversion of electromagnetic energy to heat energy also presents characteristic of thermally driven enhancement. Waste electromagnetic energy is absorbed and converted into heat energy which could be collected and reused for powering micronano devices, daily equipment or even largescale facilities. Meanwhile, the afterheat energy is also reused to power the graphene networks themselves, promoting both of the energy conversion and electromagnetic functions. This creates a good self-circulation system, which enables to recycle waste electromagnetic energy efficiently.

## 3. Conclusion

In summary, thermally driven relaxation and transport are probed experimentally and theoretically for the first time, demonstrating a competitive synergy on electromagnetic energy conversion, which transforms the negative effect of heat energy into superiority for switching self-powered and self-circulated electromagnetic devices. The link between "materials genes" and electromagnetic wave response is hierarchically dissected and visualized by a dynamic picture. A facile and generic strategy of "material genes sequencing" is successfully achieved for harvesting, converting, and reusing the waste electromagnetic energy. The electromagnetic wave absorption is thermally strengthened by ≈250% and shielding capacitor is constantly enhanced to ≈39 dB. Temperature also shifts absorption peak for 20 dB bandwidth covering the whole investigated frequency. This new finding of nonionic energy conversion takes a significant driven power to highlight recycling the waste electromagnetic energy with self-powered and self-circulated devices. They exploit a pathway for 2D materials adaptive to multifields of human livehoods, global economy, and military, including electromagnetic pollution defense and control, information security and electronic countermeasure, smart imaging, disease surveillance, thermally driven devices, and miniaerospace vehicles.

## Supporting Information

Supporting Information is available from the Wiley Online Library or from the author.

## Acknowledgements

This work was supported by the National Natural Science Foundation of China (Grant Nos. 11774027, 51132002, 11574261, 11604237, 51072024, and 51372282). The authors thank Dr. and Prof. R. C. Che (Fudan University) for technology assistance of HR-TEM.

## Conflict of Interest

The authors declare no conflict of interest.

## Keywords

charge transport, electromagnetic energy conversion, graphene, relaxation, self-power

Received: March 13, 2018
Revised: April 2, 2018
Published online:

[1] X. D. Wang, J. H. Song, J. Liu, Z. L. Wang, *Science* **2007**, *316*, 102.
[2] a) M. Zhang, T. Gao, J. S. Wang, J. J. Liao, Y. Q. Qiu, H. Xue, Z. Shi, Z. X. Xiong, L. F. Chen, *Nano Energy* **2015**, *11*, 510; b) Y. F. Lin, J. Song, Y. Ding, S. Y. Lu, Z. L. Wang, *Adv. Mater.* **2008**, *20*, 3127; c) H. J. Shin, W. M. Choi, D. Choi, G. H. Han, S. M. Yoon, H. K. Park, S. W. Kim, Y. W. Jin, S. Y. Lee, J. M. Kim, J. Y. Choi, Y. H. Lee, *J. Am. Chem. Soc.* **2010**, *132*, 15603; d) J. Kwon, W. Seung, B. K. Sharma, S. W. Kim, J. H. Ahn, *Energy Environ. Sci.* **2012**, *5*, 8970; e) Y. L. Zi, J. Wang, S. H. Wang, S. M. Li, Z. Wen, H. Y. Guo, Z. L. Wang, *Nat. Commun.* **2016**, *7*, 10987.
[3] X. Wang, Y. Yang, *Nano Energy* **2017**, *32*, 36.
[4] J. He, T. Wen, S. Qian, Z. X. Zhang, Z. M. Tian, J. Zhu, J. L. Mu, X. J. Hou, W. P. Geng, J. D. Cho, J. Q. Han, X. J. Chou, C. Y. Xue, *Nano Energy* **2018**, *43*, 326.
[5] a) M. Zhou, M. S. H. Al-Furjan, J. Zou, W. T. Liu, *Renewable Sustainable Energy Rev.* **2018**, *82*, 3582; b) K. W. Zhang, S. H. Wang, Y. Yang, *Adv. Energy Mater.* **2017**, *7*, 1601852.
[6] a) H. Y. Guo, X. M. He, J. W. Zhong, Q. Zhong, Q. Leng, C. G. Hu, J. Chen, L. Tian, Y. Xi, J. Zhou, *J. Mater. Chem. A* **2014**, *2*, 2079; b) H. Y. Shao, Z. Wen, P. Cheng, N. Sun, Q. Q. Shen, C. J. Zhou, M. F. Peng, Y. Q. Yang, X. K. Xie, X. H. Sun, *Nano Energy* **2017**, *39*, 608.
[7] a) D. Y. Kim, H. S. Kim, D. S. Kong, M. Choi, H. B. Kim, J. H. Lee, G. Murillo, M. Lee, S. S. Kim, J. H. Jung, *Nano Energy* **2018**, *45*, 247; b) L. Xu, T. Jiang, P. Lin, J. J. Shao, C. He, W. Zhong, X. Y. Chen, Z. L. Wang, *ACS Nano* **2018**, *12*, 1849; c) X. Y. Yang, S. Chan, L. Y. Wang, W. A. Daoud, *Nano Energy* **2018**, *44*, 388.
[8] a) S. Kang, H. Choi, S. Bin Lee, S. C. Park, J. B. Park, S. Lee, Y. Kim, B. H. Hong, *2D Mater.* **2017**, *4*, 025037; b) Z. G. Lu, L. M. Ma, J. B. Tan, H. Y. Wang, X. M. Ding, *2D Mater.* **2017**, *4*, 025021; c) Q. Zhang, Q. J. Liang, Z. Zhang, Z. Kang, Q. L. Liao, Y. Ding, M. Y. Ma, F. F. Gao, X. Zhao, Y. Zhang, *Adv. Funct. Mater.* **2018**, *28*, 1703801; d) J. Kang, D. Kim, Y. Kim, J. B Choi, B. H. Hong, S. W. Kim, *2D Mater.* **2017**, *4*, 025003.
[9] a) F. Shahzad, M. Alhabeb, C. B. Hatter, B. Anasori, S. M. Hong, C. M. Koo, Y. Gogotsi, *Science* **2016**, *353*, 1137; b) O. Balci, E. O. Polat, N. Kakenov, C. Kocabas, *Nat. Commun.* **2015**, *6*, 6628; c) M. K. Han, X. W. Yin, X. L. Li, B. Anasori, L. T. Zhang, L. F. Cheng, Y. Gogotsi, *ACS Appl. Mater. Interfaces* **2017**, *9*, 20038.
[10] a) S. C. Zhao, Z. Gao, C. Q. Chen, G. Z. Wang, B. Zhang, Y. Chen, J. Zhang, X. Li, Y. Qin, *Carbon* **2016**, *98*, 196; b) S. Kwon, R. Ma, U. Kim, H. R. Choi, S. Baik, *Carbon* **2014**, *68*, 118; c) X. M. Zhang, G. B. Ji, W. Liu, B. Quan, X. H. Liang, C. M. Shang, Y. Cheng, Y. W. Du, *Nanoscale* **2015**, *7*, 12932.
[11] a) Z. H. Zeng, M. J. Chen, Y. M. Pei, S. I. S. Shahabadi, B. Y. Che, P. Y. Wang, X. H. Lu, *ACS Appl. Mater. Interfaces* **2017**, *9*, 32211; b) M. H. Al-Saleh, W. H. Saadeh, U. Sundararaj, *Carbon* **2013**, *60*, 146; c) M. Arjmand, K. Chizari, B. Krause, P. Poetschke, U. Sundararaj, *Carbon* **2016**, *98*, 358.
[12] a) Z. H. Zeng, H. Jin, M. J. Chen, W. W. Li, L. C. Zhou, Z. Zhang, *Adv. Funct. Mater.* **2016**, *26*, 303; b) Y. L. Yang, M. C. Gupta, *Nano Lett.* **2005**, *5*, 2131; c) Y. Chen, H. B. Zhang, Y. B. Yang, M. Wang, A. Y. Cao, Z. Z. Yu, *Adv. Funct. Mater.* **2016**, *26*, 447; d) G. L. Wang, L. Wang, L. H. Mark, V. Shaayegan, G. Z. Wang, H. P. Li, G. Q. Zhao, C. B. Park, *ACS Appl. Mater. Interfaces* **2018**, *10*, 1195; e) Z. H. Zeng,

 © 2018 WILEY-VCH Verlag GmbH & Co. KGaA, Weinheim

H. Jin, M. J. Chen, W. W. Li, L. C. Zhou, X. Xue, Z. Zhang, *Small* **2017**, *13*, 1701388.

[13] a) H. L. Lv, X. H. Liang, G. B. Ji, H. Q. Zhang, Y. W. Du, *ACS Appl. Mater. Interfaces* **2015**, *7*, 9776; b) T. Xia, C. Zhang, N. A. Oyler, X. B. Chen, *Adv. Mater.* **2013**, *25*, 6905.

[14] a) J. W. Liu, R. C. Che, H. J. Chen, F. Zhang, F. Xia, Q. S. Wu, M. Wang, *Small* **2012**, *8*, 1214; b) G. Z. Wang, X. G. Peng, L. Yu, G. P. Wan, S. W. Lin, Y. Qin, *J. Mater. Chem. A* **2015**, *3*, 2734; c) W. B. You, H. Bi, W. She, Y. Zhang, R. C. Che, *Small* **2017**, *13*, 1602779; d) Q. H. Liu, Q. Cao, H. Bi, C. Y. Liang, K. P. Yuan, W. She, Y. J. Yang, R. C. Che, *Adv. Mater.* **2016**, *28*, 486.

[15] a) M. Rahmani, A. E. Miroshnichenko, D. Y. Lei, B. Luk'yanchuk, M. I. Tribelsky, A. I. Kuznetsov, Y. S. Kivshar, Y. Francescato, V. Giannini, M. H. Hong, S. A. Maier, *Small* **2014**, *10*, 576; b) G. Zabow, S. J. Dodd, A. P. Koretsky, *Small* **2014**, *10*, 1902; c) C. Rutherglen, P. Burke, *Small* **2009**, *5*, 884; d) H. T. Wu, S. Liu, X. Wan, L. Zhang, D. Wang, L. L. Li, T. J. Cui, *Adv. Sci.* **2017**, *4*, 1700098.

[16] a) J. C. Wang, C. S. Xiang, Q. Liu, Y. B. Pan, J. K. Guo, *Adv. Funct. Mater.* **2008**, *18*, 2995; b) G. Z. Wang, Z. Gao, S. W. Tang, C. Q. Chen, F. F. Duan, S. C. Zhao, S. W. Lin, Y. H. Feng, L. Zhou, Y. Qin, *ACS Nano* **2012**, *6*, 11009; c) N. Li, Y. Huang, F. Du, X. B. He, X. Lin, H. J. Gao, Y. F. Ma, F. F. Li, Y. S. Chen, P. C. Eklund, *Nano Lett.* **2006**, *6*, 1141; d) H. Zhou, J. C. Wang, J. D. Zhuang, Q. Liu, *Nanoscale* **2013**, *5*, 12502.

[17] a) R. C. Che, L. M. Peng, X. F. Duan, Q. Chen, X. L. Liang, *Adv. Mater.* **2004**, *16*, 401; b) S. P. Pawar, D. A. Marathe, K. Pattabhi, S. Bose, *J. Mater. Chem. A* **2015**, *3*, 656.

[18] a) G. Z. Wang, Z. Gao, G. P. Wan, S. W. Lin, P. Yang, Y. Qin, *Nano Res.* **2014**, *7*, 704; b) B. Quan, X. H. Liang, G. B. Ji, J. Lv, S. S. Dai, G. Y. Xu, Y. W. Du, *Carbon* **2018**, *129*, 310; c) Y. Zhang, Y. Huang, T. F. Zhang, H. C. Chang, P. S. Xiao, H. H. Chen, Z. Y. Huang, Y. S. Chen, *Adv. Mater.* **2015**, *27*, 2049.

[19] a) F. Sharif, M. Arjmand, A. A. Moud, U. Sundararaj, E. P. L. Roberts, *ACS Appl. Mater. Interfaces* **2017**, *9*, 14171; b) B. Shen, W. T. Zhai, W. G. Zheng, *Adv. Funct. Mater.* **2014**, *24*, 4542; c) D. X. Yan, H. Pang, B. Li, R. Vajtai, L. Xu, P. G. Ren, J. H. Wang, Z. M. Li, *Adv. Funct. Mater.* **2015**, *25*, 559; d) S. Lee, I. Jo, S. Kang, B. Jang, J. Moon, J. B. Park, S. Lee, S. Rho, Y. Kim, B. H. Hong, *ACS Nano* **2017**, *11*, 5318; e) A. A. Eddib, D. D. L. Chung, *Carbon* **2017**, *117*, 427.

[20] a) Y. Wang, W. C. Lee, K. K. Manga, P. K. Ang, J. Lu, Y. P. Liu, C. T. Lim, K. P. Loh, *Adv. Mater.* **2012**, *24*, 4285; b) S. A. Awan, A. Lombardo, A. Colli, G. Privitera, T. S. Kulmala, J. M. Kivioja, M. Koshino, A. C. Ferrari, *2D Mater.* **2016**, *3*, 015010; c) X. F. Xu, L. F. C. Pereira, Y. Wang, J. Wu, K. W. Zhang, X. M. Zhao, S. Bae, C. T. Bui, R. G. Xie, J. T. L. Thong, B. H. Hong, K. P. Loh, D. Donadio, B. W. Li, B. Oezyilmaz, *Nat. Commun.* **2014**, *5*, 3689.

[21] a) J. C. Wang, S. A. Kondrat, Y. Y. Wang, G. L. Brett, C. Giles, J. K. Bartley, L. Lu, Q. Liu, C. J. Kiely, G. J. Hutchings, *ACS Catal.* **2015**, *5*, 3575; b) R. G. Ma, X. D. Ren, B. Y. Xia, Y. Zhou, C. Sun, Q. Liu, J. J. Liu, J. C. Wang, *Nano Res.* **2016**, *9*, 808; c) Y. Wang, S. W. Tong, X. F. Xu, B. Oezyilmaz, K. P. Loh, *Adv. Mater.* **2011**, *23*, 1514; d) Y. Y. Lv, Y. Fang, Z. X. Wu, X. F. Qian, Y. F. Song, R. C. Che, A. M. Asiri, Y. Y. Xia, B. Tu, D. Y. Zhao, *Small* **2015**, *11*, 1003.

[22] a) N. Yousefi, X. Y. Sun, X. Y. Lin, X. Shen, J. J. Jia, B. Zhang, B. Z. Tang, M. S. Chan, J. K. Kim, *Adv. Mater.* **2014**, *26*, 5480; b) Q. Song, F. Ye, X. W. Yin, W. Li, H. J. Li, Y. S. Liu, K. Z. Li, K. Y. Xie, X. H. Li, Q. G. Fu, L. F. Cheng, L. T. Zhang, B. Q. Wei, *Adv. Mater.* **2017**, *29*, 1701583.

[23] J. J. Liang, Y. Wang, Y. Huang, Y. F. Ma, Z. F. Liu, J. M. Cai, C. D. Zhang, H. J. Gao, Y. S. Chen, *Carbon* **2009**, *47*, 922.

[24] B. Wen, M. S. Cao, M. M. Lu, W. Q. Cao, H. L. Shi, J. Liu, X. X. Wang, H. B. Jin, X. Y. Fang, W. Z. Wang, J. Yuan, *Adv. Mater.* **2014**, *26*, 3484.

[25] a) Z. P. Chen, W. C. Ren, L. B. Gao, B. L. Liu, S. F. Pei, H. M. Cheng, *Nat. Mater.* **2011**, *10*, 424; b) Z. P. Chen, C. Xu, C. Q. Ma, W. C. Ren, H. M. Cheng, *Adv. Mater.* **2013**, *25*, 1296.

[26] S. Singh, S. Lee, H. Kang, J. Lee, S. Baik, *Energy Storage Mater.* **2016**, *3*, 55.

[27] a) Y. S. Yun, G. Yoon, M. Park, S. Y. Cho, H. D. Lim, H. Kim, Y. W. Park, B. H. Kim, K. Kang, H. J. Jin, *NPG Asia Mater.* **2016**, *8*, e338; b) A. Hashimoto, K. Suenaga, A. Gloter, K. Urita, S. Iijima, *Nature* **2004**, *430*, 870; c) J. Lahiri, Y. Lin, P. Bozkurt, I. I. Oleynik, M. Batzill, *Nat. Nanotechnol.* **2010**, *5*, 326; d) J. C. Meyer, C. Kisielowski, R. Erni, M. D. Rossell, M. F. Crommie, A. Zettl, *Nano Lett.* **2008**, *8*, 3582.

[28] a) J. C. Meyer, A. K. Geim, M. I. Katsnelson, K. S. Novoselov, T. J. Booth, S. Roth, *Nature* **2007**, *446*, 60; b) X. Wang, L. J. Zhi, K. Muellen, *Nano Lett.* **2008**, *8*, 323.

[29] a) I. K. Moon, J. Lee, R. S. Ruoff, H. Lee, *Nat. Commun.* **2010**, *1*, 1; b) C. Gomez-Navarro, J. C. Meyer, R. S. Sundaram, A. Chuvilin, S. Kurasch, M. Burghard, K. Kern, U. Kaiser, *Nano Lett.* **2010**, *10*, 1144.

[30] N. Ghaderi, M. Peressi, *J. Phys. Chem. C* **2010**, *114*, 21625.

[31] X. Y. Fang, X. X. Yu, H. M. Zheng, H. B. Jin, L. Wang, M. S. Cao, *Phys. Lett. A* **2015**, *379*, 2245.

[32] a) S. J. Baek, W. G. Hong, M. Park, A. B. Kaiser, H. J. Kim, B. H. Kim, Y. W. Park, *Synth. Met.* **2014**, *191*, 1; b) M. S. Cao, W. L. Song, Z. L. Hou, B. Wen, J. Yuan, *Carbon* **2010**, *48*, 788; c) B. Wen, M. S. Cao, Z. L. Hou, W. L. Song, L. Zhang, M. M. Lu, H. B. Jin, X. Y. Fang, W. Z. Wang, J. Yuan, *Carbon* **2013**, *65*, 124.


© 2018 WILEY-VCH Verlag GmbH & Co. KGaA, Weinheim